Article:
Johnston, B.I.J. orcid.org/0000-0002-3586-1682, Baker, P.J. and Cussen, S.A. orcid.org/0000-0002-9303-4220 (2021) Ion dynamics in fluoride-containing polyatomic anion cathodes by muon spectroscopy. Journal of Physics: Materials, 4 (4). 044015. ISSN 2515-7639

https://doi.org/10.1088/2515-7639/ac22ba

JPhys Materials

Ion dynamics in fluoride-containing polyatomic anion cathodes by muon spectroscopy

IOP Publishing J. Phys. Mater. 4 (2021) 044015 https://doi.org/10.1088/2515-7639/ac22ba

Journal of Physics: Materials

OPEN ACCESS

RECEIVED
27 May 2021

REVISED
18 August 2021

ACCEPTED FOR PUBLICATION
1 September 2021

PUBLISHED
13 September 2021

PAPER

Ion dynamics in fluoride-containing polyatomic anion cathodes by muon spectroscopy

Beth I J Johnston[1,4,*], **Peter J Baker**[3,4] **and Serena A Cussen**[1,2,4,*]

[1] Department of Chemical and Biological Engineering, The University of Sheffield, Sir Robert Hadfield Building, Sheffield S1 3JD, United Kingdom
[2] Department of Materials Science and Engineering, The University of Sheffield, Sir Robert Hadfield Building, Sheffield S1 3JD, United Kingdom
[3] ISIS Pulsed Neutron and Muon Source, STFC Rutherford Appleton Laboratory, Harwell Science and Innovation Campus, Didcot, Oxfordshire OX11 0QX, United Kingdom
[4] The Faraday Institution, Quad One, Harwell Science and Innovation Campus, Didcot OX11 0RA, United Kingdom
[*] Authors to whom any correspondence should be addressed.

E-mail: beth.johnston@sheffield.ac.uk **and** s.cussen@sheffield.ac.uk

Keywords: Na-ion cathode, Li-ion cathode, muon spin relaxation spectroscopy, ion diffusion

Supplementary material for this article is available online

Abstract

Polyatomic anion insertion electrodes present compositional and morphological variety, as well as the ability to tune operational voltages by influencing the nature of metal-oxygen bonding. Realizing the application of these compounds as electrodes in Li- and Na-ion batteries requires a detailed understanding of ion dynamics in these systems. Here is presented the microscopic Li-ion and Na-ion diffusion properties in $LiFeSO_4F$ and Na_2FePO_4F, respectively, using muon spin relaxation (μ^+SR) spectroscopy for the first time. Li-ion diffusion processes in the tavorite $LiFeSO_4F$ phase are found to proceed with an activation energy (E_a) of 48(4) meV and a diffusion coefficient of 1.71×10^{-9} cm^2 s^{-1}, while Na-ion mobility in Na_2FePO_4F has a calculated diffusion coefficient of 3.47×10^{-10} cm^2 s^{-1} and a higher energy barrier to ion diffusion at 96(8) meV. This is the first such examination of fluoride-containing polyatomic cathodes using μ^+SR, where the presence of the highly electronegative fluoride species was thought to preclude activation energy and diffusion coefficient determination due to strong μ^+-F^- interactions. These insights open up the possibility of studying a myriad of fluoride-containing electrode materials using the μ^+SR technique.

1. Introduction

The design of high energy density electrode materials is essential to meet the demands of battery-powered electrified transport. Great emphasis has been placed on cathode developments, where polyatomic anion cathodes have garnered much interest since electrochemical activity in $LiFePO_4$ was first reported, where the rigid P–O bonds impart excellent thermal stabilities and furthermore act to raise the operating potential of the cell through means of the inductive effect [1]. The rich compositional variety offered by different polyanionic moieties allows for the tailoring of operating potentials and the resulting electrochemical properties. For example, replacement of the $(PO_4)^{3-}$ group with the more electronegative $(SO_4)^{2-}$ group in the NASICON-type frameworks $Li_2Fe_3(PO_4)_3$ and $Fe_2(SO_4)_3$ effects a 0.8 eV increase in the open-circuit voltage [2]. Considering the success of $LiFePO_4$ as a cathode material, the Fe-containing fluorosulphate $LiFeSO_4F$ has received considerable attention owing to the strong electron-withdrawing behavior of both the $(SO_4)^{2-}$ group and the singly-charged fluoride anion which serve to significantly increase the observed potential; the triplite phase $LiFeSO_4F$ displays an Fe^{2+}/Fe^{3+} redox potential of 3.9 V [3]. The tavorite phase of this material, which is more easily synthesized, displays a redox potential of 3.6 V and is still an attractive option for higher voltage polyatomic anion cathodes [4]. Computational analysis suggests a low activation energy (≈0.4 eV) for Li^+ mobility and AC and DC conductivity measurements indicate higher Li^+ diffusion

coefficients for $LiFeSO_4F$ compared to $LiFePO_4$ [4, 5]. Here, we report, for the first time, the local-scale diffusive nature of Li^+ within the tavorite $LiFeSO_4F$ material by use of muon spin relaxation (μ^+SR) spectroscopy. μ^+SR has been widely applied to study dynamic and static properties in functional materials, where the interactions between the muon spin and internal magnetic fields can yield valuable information on molecular dynamics, superconductivity, and magnetism [6]. There has been increasing interest in applying the μ^+SR method for studying Li^+ diffusional behavior across a range of Li-ion battery cathodes such as $LiFePO_4$, $LiCoO_2$ and $LiNi_{1/3}Mn_{1/3}Co_{1/3}O_2$, owing to the ability of the muon to act as a local-scale probe overcoming sensitivities related to surface effects and grain boundaries [7–10]. Furthermore, the μ^+SR technique is not limited to the study of Li^+ diffusion, and any species with a non-zero nuclear magnetic moment can act to perturb the muon spin. This is highly relevant in energy materials where technologies utilizing cheaper, more abundant cations such as Na^+ and Mg^{2+} are primed to complement Li-ion batteries [11]. In particular, Na-ion batteries are poised to lead these alternative technologies, where the lower energy densities (attributed to the heavier, larger Na^+ cation and the *ca.* 0.3 V decrease between the Li/Li^+ and Na/Na^+ redox couples) are well suited for stationary energy storage applications [12]. The diffusive behavior of Na^+ cations has also been studied using μ^+SR including olivine $NaFePO_4$, $NaMn_2O_4$ and $NaCoO_2$ [13–15]. Similarly to materials for Li-ion materials, there is also an interest in polyatomic anion based Na-ion cathodes such as layered Na_2FePO_4F, which interestingly presents two-dimensional Na^+ diffusion [16]. Up to now, the μ^+SR technique has not been applied to battery materials containing fluoride ions since spin polarized positive muons can bind strongly to fluoride ions to form a number of species such as F-μ-F and F-μ [17, 18]. Since the most likely muon stopping site is close to the electronegative fluoride ion, there remains the question of whether strong binding between these will preclude observation of any effects by diffusing Li^+ or Na^+ ions near that stopping site. On the other hand, this binding interaction could place the muon in a prime location to effectively 'see' the nearby diffusing ions and present an interesting hypothesis worth testing.

Although such binding is generally only studied at low temperatures, the question remained open as to whether these species would affect ion dynamics measurements. Polytetrafluoroethylene is a good example of a material with well-defined F-μ-F oscillations at low temperature that disappear at higher temperatures due to molecular dynamics effects. However, such molecular effects would not occur in the inorganic crystalline frameworks generally used for applications such as rechargeable battery electrodes. More generally, F-μ-F oscillations do disappear at higher temperatures, and this has been assumed to be muon diffusion, however experimental evidence of muon hopping in fluoride materials is limited [19, 20]. Calculations of the binding energy for the muons have been carried out on simple fluorides but for materials such as $LiFeSO_4F$ and Na_2FePO_4F such calculations are likely to be challenging because of the significantly larger number of atoms per unit cell [18, 21]. Experimental evidence demonstrating the ability to observe ion dynamics using muons in fluorine containing structures would therefore be useful.

2. Results and discussion

Conventional high temperature synthesis routes to tavorite $LiFeSO_4F$ are limited owing to its low decomposition temperature (~400 °C) and the high solubility in water further precludes the application of aqueous synthetic strategies. Solvothermal or microwave-assisted strategies utilizing polyol media have successfully delivered the tavorite phase [22, 23]. In the case of the low temperature microwave-assisted solvothermal route adopted here (and adapted from that reported by Tripathi *et al* [23]), rapid and uniform heating of the liquid medium through the microwave dielectric heating effect is achieved by the use of a tetraethylene glycol solvent. Powder x-ray diffraction (PXRD) data collected for the synthesized $LiFeSO_4F$ sample indicates the tavorite phase is obtained. Figure S1 (available online at stacks.iop.org/JPMATER/4/044015/mmedia) shows the results obtained from Rietveld refinement using a *P-1* structural model fit to the collected PXRD data. An additional *Fm-3m* phase was also included to account for small quantities of LiF remaining in the final product and phase and weight fractions of LiF were calculated as 0.25% and 0.1% respectively. The refined unit cell parameters, alongside statistical agreement factors R_{wp} and χ^2 are shown in table S1. Calculated lattice parameters show good agreement with comparable data in the literature.

The microscopic Li^+ diffusion within the tavorite $LiFeSO_4F$ framework was analyzed using μ^+SR where a positively charged muon acts as a sensitive local-scale probe for both internal static magnetic fields, and dynamic fields arising from diffusing Li^+ cations. Both naturally occurring Li isotopes possess non-zero spin (thus non-zero nuclear magnetic moments), making them excellent candidates to be studied using μ^+SR. In a typical μ^+SR experiment, spin polarized muons are implanted into the sample where they stop at interstitial sites close to regions of high electron density.

While implanted, the muon spin direction experiences a local field distribution (Δ) caused by surrounding static nuclear magnetic environments and a fluctuation rate (ν) induced by the motion of

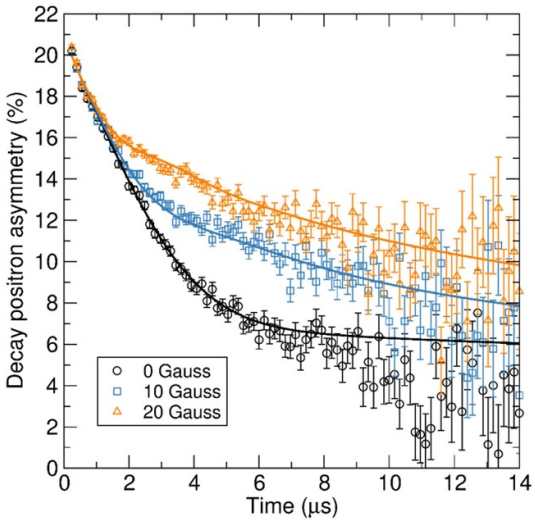

Figure 1. Raw μ^+SR data obtained for tavorite $LiFeSO_4F$ at 300 K at ZF and applied LFs of 10 G and 20 G. Solid lines correspond to the fits obtained using the dynamic KT function.

surrounding nuclei. In the case of lithium and sodium ion cathodes, ν is largely affected by Li^+ or Na^+ diffusion respectively. These effects serve to perturb the muon spin, with a resultant depolarization of the spin ensemble over time. With a mean lifetime of 2.2 μs the implanted muon decays into a positron and two neutrinos via a three-body process governed by the weak interaction. As a result of this, parity conservation is violated and the positron is emitted preferentially in the same direction as the muon spin direction at the instant of decay [6]. Thus, the time evolution of the positron asymmetry is directly linked to the time evolution of the muon spin relaxation which in itself reveals the ion dynamics in the system. The positron asymmetry $A(t)$ can be deduced by considering the counts of detected positrons in forward (N_F) and backward (N_B) (relative to the incoming muon beam) detector banks placed around the sample such that

$$A(t) = \frac{N_F(t) - \alpha N_B(t)}{N_F(t) + \alpha N_B(t)}$$

where α is a correction factor to compensate for efficiency discrepancies between the two detectors.

Muon measurements for the $LiFeSO_4F$ sample were taken at intervals of 20 K in the temperature range 100 K to 400 K at zero field (ZF) and applied longitudinal fields (LFs) of 10 and 20 G. The raw data obtained for these measurements at 300 K are shown in figure 1 and represent the time evolution of the decay positron asymmetry. It is observed that this asymmetry initially undergoes a rapid relaxation, followed by a slower relaxation at longer times. The initial relaxation is independent of the applied magnetic field and represents the interactions between the muon spin and magnetic moments arising from the *d*-electrons of the Fe^{2+} cations. The latter slower relaxation is caused by interactions between the muon spin ensemble and the surrounding nuclear magnetic moments of atomic isotopes with a non-zero spin e.g. ^{6}Li, ^{7}Li, ^{57}Fe and ^{19}F. Upon the application of stronger LFs, the relaxation rate becomes slower through the decoupling of the muon spin from the static nuclear magnetic moments. The muon decay asymmetry data at each temperature were fitted with the WiMDA program, using a dynamic Kubo-Toyabe (KT) function to obtain the muon spin fluctuation rate, ν, arising from Li^+ diffusion [24]. The data were fit using a baseline asymmetry to account for the background and an exponentially relaxing signal accounting for initial fast relaxation from the paramagnetic iron multiplying the dynamical form of the KT function that describes the dynamic nuclear magnetic fields, such that

$$A_0 P(t) = A_{bg} + A_{KT} P_{KT}(\Delta, \nu, t)\, e^{-\lambda t}$$

where A_{bg} and A_{KT} are the respective amplitudes of the two components and P_{KT} is the dynamic KT function, which is sensitive to the trend of the static field distribution width (Δ) and the field fluctuation rate (ν) with time (t). For both samples studied here, the KT function was fit to all three datasets (ZF, 10 G LF and 20 G LF) simultaneously in order to isolate the contribution to the asymmetry signal from Li^+ hopping, and lead to more reliable determinations of ν and Δ parameters.

The temperature dependence of ν over the applied temperature range is shown in figure 2(a). This fluctuation rate provides information on the Li^+ hopping rates. From the values obtained from the data

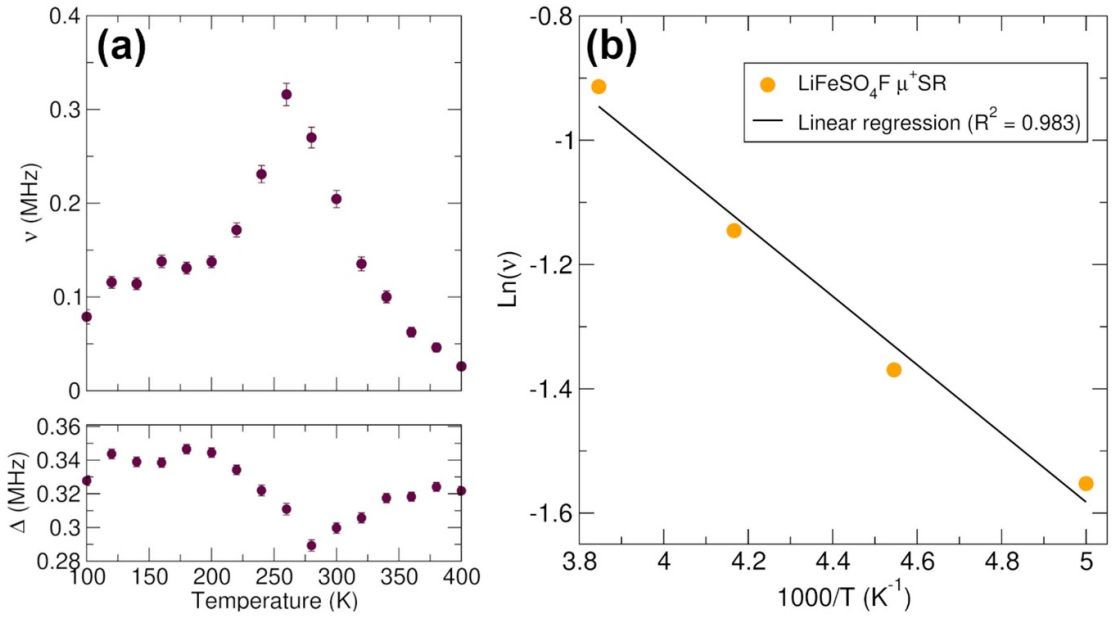

Figure 2. (a) Temperature dependence of ν and Δ obtained from μ^+SR data obtained for tavorite $LiFeSO_4F$ fit using a dynamic KT function and (b) Arrhenius plot of v over the thermally activated region calculated with a calculated E_a of 48(4) meV.

fitting, it can be seen that ν values remain steady until a sharp increase is observed in the 200 K to 260 K region which represents the onset of thermally activated Li^+ diffusion. The thermally activated region is followed by a sharp drop after 260 K, a trend that is often observed in μ^+SR studies of ionic conduction in cathode materials, and is thought to represent the point where Li^+ diffusion becomes too fast to be detected by μ^+SR (see also figure S5). The temperature dependence of Δ shows a relatively stable region between 100 to 180 K before decreasing over the thermally activated region by ≈0.06 MHz which could be attributed to motional narrowing arising from faster Li^+ hopping between sites. This trend is also observed in $LiFePO_4$ [8, 25, 26]. The subsequent smaller increase in Δ at higher temperatures suggests that some part of the field distribution remains absent due to motional narrowing. Other potential origins for this behavior could be muons distributed across two stopping sites close to both O^{2-} and F^- anions, with the F^- anion playing a role in the deviation from commonly observed trends. It could also be explained by small structural rearrangements e.g. oxygen or fluorine displacements near the muon stopping sites. However, similar trends have also been observed in μ^+SR experiments carried out by Vidal Laveda *et al* for cathode materials $LiFe_{0.5}Mn_{0.5}PO_4$ and $LiFe_{0.25}Mn_{0.75}PO_4$, where Δ increases by a similar value (∼0.02–0.04 MHz) towards higher temperatures [27]. To calculate the activation energy, E_a, of ion diffusion, a plot of $\ln(\nu)$ vs. $1/T$ (figure 2(b)) is constructed over the thermally activated region where E_a can be calculated from the gradient of the straight line fit according to equation (1):

$$\ln(\nu) = \frac{-E_a}{k_B T} + \ln(A) \tag{1}$$

where k_B is the Boltzmann constant (1.38×10^{-23} J K^{-1}), and A is the pre-exponential factor associated with the Arrhenius equation.

An E_a of 48 ± 4 meV was estimated for tavorite $LiFeSO_4F$, which compares well with values reported for other polyatomic anion materials using μ^+SR e.g. E_a for microwave-synthesized $LiFePO_4$ and $LiFe_{1-x}Mn_xPO_4$ were calculated to be in the range of 46–122 meV [8, 27]. By considering ion motion along the [111] direction within the $LiFeSO_4F$ structure, predicted to be the most favorable pathway for Li^+ transport, the diffusion coefficient D_{Li} can be estimated by applying equation (2), where the contribution from individual jumps in the diffusion pathway under consideration can be summed where N_i represents the number of accessible Li^+ sites in the ith jump, $Z_{c,i}$ is the vacancy fraction of the destination site, s_i is the jump distance and ν is the field fluctuation rate obtained from data fitting:

$$D_{Li} = \sum_{i=1}^{n} \frac{1}{N_i} Z_{\nu,i} s_i^2 \nu. \tag{2}$$

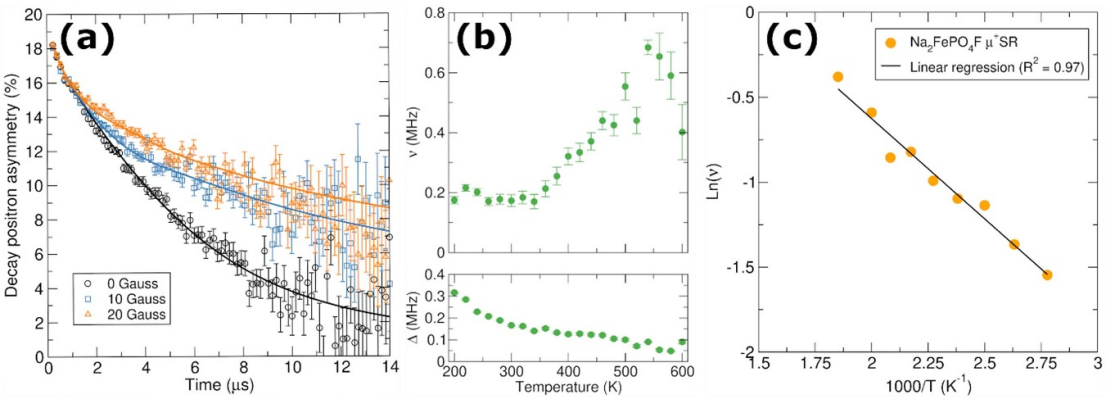

Figure 3. (a) Raw μ^+SR data obtained for Na_2FePO_4F at 300 K at ZF and LFs of 10 G and 20 G. Solid lines correspond to the fits obtained using the dynamic KT function. (b) Temperature dependence of ν and Δ obtained from μ^+SR data for Na_2FePO_4F, fit using a dynamic KT function and (c) Arrhenius plot of v over the thermally activated region calculated $E_a = 96(8)$ meV.

This transport pathway consists of two jumps of length 3.91 Å and 4.22 Å which form a zig-zag pathway that propagates along the [111] direction and forming an open 1D tunnel for Li^+ diffusion (figure S2). By extrapolation of the line of best fit (figure 2(b)) to obtain a value for ν at 300 K, a room temperature D_{Li} of 1.71×10^{-9} cm^2 s^{-1} is calculated for tavorite $LiFeSO_4F$. This matches well with D_{Li} values predicted by atomistic modeling that are estimated to be between 10^{-10} and 10^{-8} cm^2 s^{-1} [5]. This also compares well with room temperature D_{Li} values calculated using μ^+SR for $LiFe_{1-x}Mn_xPO_4$ ($D_{Li} = 2.0 \times 10^{-10}$–$6.25 \times 10^{-10}$ cm^2 s^{-1}) and suggests enhanced diffusion kinetics for $LiFeSO_4F$.

The local diffusion properties of Na^+ within the Na_2FePO_4F framework has also been investigated here using μ^+SR, where the 100% abundance of ^{23}Na with a spin of +3/2 allows for a similar procedure to be followed. The material was synthesized using a solid-state method detailed in the SI with the Na_2FePO_4F *Pbcn* structure confirmed using PXRD and Rietveld refinement (figure S3). Calculated lattice parameters (table S2) show good agreement with previously reported literature values [28, 29]. Muon measurements for Na_2FePO_4F were taken at intervals of 20 K in the temperature range 200 K to 600 K at ZF and applied LFs of 10 and 20 G. The raw muon data collected at 300 K (figure 3(a)) shows features of paramagnetic and nuclear relaxation processes, similar to what was observed previously in $LiFeSO_4F$. The data were fit using a dynamic KT function to yield the temperature dependence of ν (figure 3(b)). The onset of thermal diffusion is notably higher in this sample compared to $LiFeSO_4F$ which is logical considering the heavier and larger Na^+ cation compared to Li^+ (see also figure S6). The temperature dependence of Δ shows a general trend of a steady decrease, as a result of motional narrowing effects as increase in temperature cause faster Na^+ hopping rates. To calculate the E_a for ion diffusion, the region between 360 K and 540 K was analyzed. The Arrhenius analysis is shown in figure 3(c), where an E_a of 96(8) meV can be estimated from the gradient. In comparison to other Na-containing materials studied using μ^+SR, the E_a is of similar magnitude to those reported in the literature. For example, E_a for Na^+ diffusion in $Na_{1.5}La_{1.5}TeO_6$, $NaMn_2O_4$ and NaV_2O_4 were estimated to be 163, 180 and 225 meV respectively while $Na_{0.7}CoO_2$ was calculated to have an E_a of 478 meV [14, 15, 30, 31]. It is also noted that activation barriers for Na^+ diffusion are often larger than those values commonly obtained for Li-containing cathode materials (e.g. $E_a = 48$ meV for $LiFeSO_4F$), indicating more sluggish diffusion kinetics for Na^+ diffusion. By considering diffusion along both the [100] and [001] directions (figure S4), the diffusion coefficient for Na^+ mobility in Na_2FePO_4F can be calculated from equation (2) as $D_{Na[100]} = a^2\nu/8$ and $D_{Na[001]} = c^2\nu/8$ where a and c are the lattice parameters derived from Rietveld refinements, $N_{[100]} = 2$, $s_{[100]} = a/2$, $N_{[001]} = 2$, $s_{[001]} = c/2$ and ν is the field fluctuation rate obtained from the μ^+SR fits. This models the Na^+ ions hopping to interstitial sites along each channel. Therefore, the diffusion coefficients can be estimated at 300 K as $D_{Na[100]} = 5.71 \times 10^{-11}$ cm^2 s^{-1} and $D_{Na[001]} = 2.90 \times 10^{-10}$ cm^2 s^{-1} with a combined diffusion coefficient of $D_{Na} = 3.47 \times 10^{-10}$ cm^2 s^{-1}. The values presented here compare favorably with other results presented in the literature, for example room temperature coefficients of 3.99×10^{-11} cm^2 s^{-1} and 1.1×10^{-11} cm^2 s^{-1} were calculated for $Na_{0.7}CoO_2$ and $NaMn_2O_4$ using μ^+SR.

3. Conclusions

In conclusion, we have successfully demonstrated the application of the μ^+SR technique to measure the microscopic ionic diffusion in fluorine containing polyatomic anion cathode materials $LiFeSO_4F$ and

Na_2FePO_4F. Activation energies of 48(4) meV and 96(8) meV were calculated for these respectively, alongside room temperature ion diffusion coefficients of $D_{Li} = 1.71 \times 10^{-9}$ cm^2 s^{-1} and $D_{Na} = 3.47 \times 10^{-10}$ cm^2 s^{-1}. These findings highlight the promising transport properties of both cathode materials, as well as the versatility of the μ^+SR technique for probing different diffusing ions [32]. Interestingly, the ability to successfully apply μ^+SR in the examination of materials containing the strongly electronegative fluoride ion extends the application of muons to new polyatomic anion materials of increasing interest for energy storage applications.

To fully exploit the potential of fast ion dynamics in energy storage materials, it is critical to develop a detailed understanding of the transport mechanisms in these functional materials. The work presented here both highlights the ability of μ^+SR to probe ion dynamics in fluorinated frameworks and provides a quantitative description of these dynamics to make meaningful comparisons to similar systems. Extending the range of materials that can be studied by μ^+SR is important for developing a detailed understanding across the myriads of competing structures for next generation energy storage applications. This is especially relevant for the fluoride containing polyatomic anion cathodes examined here, which offer increased operating potentials and improved safety as a result of the polyatomic moieties present. Furthermore, these Fe-based systems present a more sustainable and environmentally benign solution compared to Ni and Co based systems that are prevalent in most current commercial Li-ion batteries. The findings presented here highlight the promising transport properties of both cathode materials when compared with similar systems, as well as the versatility of the μ^+SR technique for probing different diffusing ions.

Data availability statement

The data that support the findings of this study are available upon reasonable request from the authors.

Acknowledgements

The authors gratefully acknowledge the STFC for the allocation of beamtime at the EMU beamline at the ISIS Neutron and Muon Souce and funding support from the Faraday Institution [Grant Nos. FIRG017, FIRG018], the Engingeering and Physical Sciences Research Council [EPSRC, EP/N001982/2] and The Carnegie Trust for the Universities of Scotland.

ORCID iDs

Beth I J Johnston https://orcid.org/0000-0002-3586-1682
Peter J Baker https://orcid.org/0000-0002-2306-2648
Serena A Cussen https://orcid.org/0000-0002-9303-4220

References

[1] Padhi A K, Nanjundaswamy K S and Goodenough J B 1997 *J. Electrochem. Soc.* **144** 1188
[2] Padhi A K, Manivannan V and Goodenough J B 1998 *J. Electrochem. Soc.* **145** 1518
[3] Ati M, Melot B C, Chotard J N, Rousse G, Reynaud M and Tarascon J M 2011 *Electrochem. Commun.* **13** 1280
[4] Recham N, Chotard J N, Dupont L, Delacourt C, Walker W, Armand M and Tarascon J M 2010 *Nat. Mater.* **9** 68
[5] Tripathi R, Gardiner G R, Islam M S and Nazar L F 2011 *Chem. Mater.* **23** 2278
[6] Blundell S J 1999 *Contemp. Phys.* **40** 175
[7] Sugiyama J *et al* 2011 *Phys. Rev.* B **84** 054430
[8] Ashton T E, Laveda J V, MacLaren D A, Baker P J, Porch A, Jones M O and Corr S A 2014 *J. Mater. Chem.* A **2** 6238
[9] Sugiyama J, Mukai K, Ikedo Y, Nozaki H, Månsson M and Watanabe I 2009 *Phys. Rev. Lett.* **103** 147601
[10] Månsson M, Nozaki H, Wikberg J M, Prša K, Sassa Y, Dahbi M, Kamazawa K, Sedlak K, Watanabe I and Sugiyama J 2014 *J. Phys.: Conf. Ser.* **551** 012037
[11] Bayliss R D *et al* 2020 *Chem. Mater.* **32** 663
[12] Hwang J Y, Myung S T and Sun Y K 2017 *Chem. Soc. Rev.* **46** 3529
[13] Sugiyama J, Nozaki H, Umegaki I, Harada M, Higuchi Y, Ansaldo E J, Brewer J H, Miyake Y, Kobayashi G and Kanno R 2014 *J. Phys.: Conf. Ser.* **551** 012012
[14] Umegaki I, Nozaki H, Harada M, Månsson M, Sakurai H, Kawasaki I, Watanabe I and Sugiyama J 2018 *JPS Conf. Proc.* **21** 011018
[15] Månsson M and Sugiyama J 2013 *Phys. Scr.* **88** 068509
[16] Ellis B L, Makahnouk W R M, Makimura Y, Toghill K and Nazar L F 2007 *Nat. Mater.* **6** 749
[17] Möller J S *et al* 2013 *Phys. Scr.* **88** 068510
[18] Möller J S, Ceresoli D, Lancaster T, Marzari N and Blundell S J 2013 *Phys. Rev.* B **87** 121108
[19] Brewer J H, Harshman D R, Keitel R, Kreitzman S R, Luke G M, Noakes D R, Turner R E and Ansaldo E J 1986 *Hyperfine Interact.* **32** 677
[20] Attenborough M, Hall I, Nikolov O, Brown S R and Cox S F J 1996 *Phys. Rev.* B **54** 6448
[21] Bernardini F, Bonfà P, Massidda S and De Renzi R 2013 *Phys. Rev.* B **87** 115148
[22] Tripathi R, Ramesh T N, Ellis B L and Nazar L F 2010 *Angew. Chem. Int. Ed.* **49** 8738

[23] Tripathi R, Popov G, Sun X, Ryan D H and Nazar L F 2013 *J. Mater. Chem.* A **1** 2990
[24] Pratt F 2000 *Physica* B **289–290** 710
[25] Sugiyama J *et al* 2012 *Phys. Rev.* B **85** 054111
[26] Baker P J, Franke I, Pratt F L, Lancaster T, Prabhakaran D, Hayes W and Blundell S J 2011 *Phys. Rev.* B **84** 174403
[27] Laveda J V, Johnston B, Paterson G W, Baker P J, Tucker M G, Playford H Y, Jensen K M Ø, Billinge S J L and Corr S A 2018 *J. Mater. Chem.* A **6** 127
[28] Tripathi R, Wood S M, Islam M S and Nazar L F 2013 *Energy Environ. Sci.* **6** 2257
[29] Ellis B L, Michael Makahnouk W R, Rowan-Weetaluktuk W N, Ryan D H and Nazar L F 2010 *Chem. Mater.* **22** 1059
[30] Amores M, Baker P J, Cussen E J and Corr S A 2018 *Chem. Commun.* **54** 10040
[31] Månsson M, Umegaki I, Nozaki H, Higuchi Y, Kawasaki I, Watanabe I, Sakurai H and Sugiyama J 2014 *J. Phys.: Conf. Ser.* **551** 012035
[32] McClelland I, Johnston B, Baker P J, Amores M, Cussen E J and Corr S A 2020 *Annu. Rev. Mater. Sci* **50** 371